Available online at www.sciencedirect.com
SCIENCE DIRECT®
International Journal of Heat and Mass Transfer 49 (2006) 2984–2994
International Journal of HEAT and MASS TRANSFER
www.elsevier.com/locate/ijhmt

Intrinsic verification methods in linear heat conduction

James V. Beck [a,*], Robert McMasters [b], Kevin J. Dowding [c], Donald E. Amos [d]

[a] Department of Mechanical Engineering (Prof. Em.), Michigan State University, E. Lansing, MI 48824, United States
[b] Department of Mechanical Engineering, Virginia Military Institute, Lexington, VA 24450, United States
[c] Sandia National Laboratories, Albuquerque, NM 87185, United States
[d] Sandia National Laboratories (Retired), Albuquerque, NM 87185, United States

Received 11 July 2005; received in revised form 20 January 2006
Available online 24 April 2006

Abstract

Verification of the codes that provide numerical heat transfer solutions obtained by finite difference and other methods is important. One way to verify these solutions is to compare the values with exact solutions. However, these exact solutions should also be verified. Fortunately, intrinsic verification methods are possible. Intrinsic verification utilizes at least two independent exact solutions to obtain accurate numerical values. Three different types of intrinsic verification for transient and steady state heat conduction are developed and illustrated by examples.

Keywords: Intrinsic verification; Time partitioning; Analytical heat conduction; Exact

1. Introduction

Verification of approximate, multi-dimensional numerical solutions in heat transfer is becoming an important research area. The accuracy of solutions from finite element, finite control volume and other methods for known partial differential equations needs to be assured. One way to do that is to compare the numerical values found using such methods with exact values. Two ways to generate the requisite exact solutions are through the use of (a) manufactured solutions and (b) exact solutions for basic geometries with simple boundary conditions in transient heat conduction. Manufactured solutions [1–3] have the advantage of being applicable for both linear and nonlinear problems but may need source terms to satisfy the partial differential equation; the boundary conditions are not specified a priori but are determined by the assumed manufactured solution. The resulting source terms and boundary conditions tend to be complicated functions of space and time. Exact transient heat conduction solutions [4,5] are usually restricted to linear cases but the boundary conditions, initial condition and volumetric energy generation term can be specified. The geometries are limited to basic shapes, such rectangles and parallelepipeds.

A major purpose of this paper is to demonstrate that many exact transient heat conduction solutions contain the possibility of intrinsic verification. To some extent, this paper reveals the *discovery* of unique verification potentials of exact solutions. We use the words "intrinsic verification" to mean the determination of the correct numerical value, to many significant figures, in two or more independent ways. In two major types of intrinsic verification methods (IVMs), a quantity exists which can be varied over an acceptable range while giving the "same" numerical value. It is a very fortunate characteristic because IVMs provide means to verify the exact solutions used for code verification. Intrinsic verification methods can be applicable to a variety and range of problems other than heat conduction.

Exact solutions must satisfy the governing partial differential equation and also the boundary and initial

* Corresponding author. Tel.: +1 517 349 6688; fax: +1 517 353 1750.
E-mail address: beck@egr.msu.edu (J.V. Beck).

0017-9310/$ - see front matter © 2006 Elsevier Ltd. All rights reserved.
doi:10.1016/j.ijheatmasstransfer.2006.01.045

Nomenclature

B	boundary condition modifier, used in case identification number system
C	dimensionless cutoff time
G	Green's function (m^{-1}, for 1D form, m^{-3} for 3D)
k	thermal conductivity (W/m °C)
L	edge dimension of a cube (m)
q_0	prescribed heat flux at a boundary (W/m^2)
t	time (s)
T	temperature (°C)
u	cotime variable, $t-\tau$ (s)
x, y, z	spatial variables (m)
X, Y, Z	denotes x-direction Cartesian geometry, used in case numbering system

Greek symbols

α	thermal diffusivity (m^2/s)
β	eigenvalue in the x-direction
γ	eigenvalue in the y-direction
η	eigenvalue in the z-direction
τ	dummy time variable (s)
ϕ	norm of eigenvalues

Subscripts

1D	one-dimensional
c.t.	complementary transient
m, n, p	counting integers for eigenvalues in the x, y, and z directions, respectively
0	constant value or cutoff time
p	partition time

Superscripts

L	long cotime
S	short cotime

conditions. However, analytical checks of these conditions might not reveal certain errors. For example, the eigenvalues might not be accurate or an eigenvalue might be missing. It is also possible that convergence of series may be so poor that accurate values are not obtainable. Sometimes an insufficient number of terms in the infinite series may be used. By using IVMs we can quantitatively and confidently check the accuracy of the numerical values generated by exact solutions. We have used these concepts in developing computer codes and have (intrinsically) verified literally thousands of exact transient heat conduction solutions involving parallelepipeds.

Three different types of intrinsic verification are considered herein. They are not all new but this is the first paper to identify all three as being IVMs. The first type, described in Section 2, is related to time partitioning [5–10] in which varying a partition time changes numerical values in a minimal fashion. In fact, these small changes indicate the accuracy of the numerical values. This first IVM uses Green's functions coming from both the Laplace transform and separation of variables. The second IVM is given in Section 3 which uses different methods of solution for steady state problems; it does not have a parameter that can be continuously varied and yet get the "same" numerical value. Instead different solutions of the same problem are found and compared. The third IVM, described in Section 4, uses only the Green's functions coming from separation of variables; like the first IVM, it has a parameter which can be varied to demonstrate verification. This third IVM is particularly appropriate for locations removed from the heated surface where the temperature is known to be zero (or as close as desired) for sufficiently small times. A second variation of this third IVM uses 1D solutions for short times.

2. The first IVM: time-partitioning intrinsic verification

The time-partitioning IVM is illustrated by considering a 3D example. Consider a cube, L on a side, which is heated by a constant heat flux, q_0, at $x=0$ and all the other surfaces are held at temperature of zero. The initial temperature throughout the cube is also zero. The describing heat conduction equation, boundary conditions and initial condition are

$$\frac{\partial^2 T}{\partial x^2}+\frac{\partial^2 T}{\partial y^2}+\frac{\partial^2 T}{\partial z^2}=\frac{1}{\alpha}\frac{\partial T}{\partial t}, \quad 0<x<L, \quad 0<y<L, \quad 0<z<L, \quad t>0 \tag{1}$$

$$-k\frac{\partial T}{\partial x}(0,y,z,t)=q_0, \quad T(L,y,z,t)=0, \quad T(x,0,z,t)=0, \quad T(x,L,z,t)=0, \quad T(x,y,0,t)=0, \quad T(x,y,L,t)=0, \quad T(x,y,z,0)=0 \tag{2}$$

The symbol T is the temperature; α is the thermal diffusivity and k is the thermal conductivity. Using the number system given in [5], this problem is denoted $X21B10$ $Y11B00$ $Z11B00T0$. (The X, Y and Z denote the x-, y- and z-directions; $X21$ denotes a boundary condition of the second kind (prescribed heat flux at $x=0$) and a boundary condition of the first kind (prescribed temperature) at $x=L$. Two other kinds of boundary conditions are convective, called the third kind and denoted with a 3, and zeroth kind which designates a condition at infinity for Cartesian coordinates. The B denotes a boundary condition modifier with $B10$ indicating a constant, but nonzero, condition at $x=0$ and a zero value at $x=L$. $T0$ indicates zero initial temperature.) The problem given by Eqs. (1) and (2) can be solved exactly in several ways. The most common is to use the

method of separation of variables (SOV); this is usually accomplished by first solving for the steady state component of the solution, the negative of which is used as the initial condition for the transient component of the solution. We have called this transient solution component the "complementary transient solution" [8,9]. Another method of solution uses the Laplace transform. The SOV method is particularly effective for large dimensionless times when fewer terms of the series are needed. The Laplace transform solution is most effective (fewer terms needed and better accuracy) for small dimensionless times. The time-partitioning method uses components of both the SOV and the Laplace transform methods. Although approaches other than Green's functions might be used for the time-partitioning method, we have found that it is convenient to use them.

The solution for the temperature in the above problem using Green's functions is [5]:

$$T(x,y,z,t) = \frac{\alpha}{k} q_0 \int_{u=0}^{t} G_{X21}(x,0,u) \int_{y'=0}^{L} G_{Y11}(y,y',u)\,\mathrm{d}y' \times \int_{z'=0}^{L} G_{Z11}(z,z',u)\,\mathrm{d}z'\,\mathrm{d}u \tag{3}$$

where u is a variable which we call the "cotime" [8,9]. The Green's function, G, is the temperature response at a location (x,y,z) and time t caused by an instantaneous source at (x',y',z') and time τ. Cotime, u, is equal to $t-\tau$. In the time-partitioning solution Eq. (3) is written in two parts, one for the short cotimes and the other for the long cotimes as

$$\begin{aligned} T(x,y,z,t) = {} & \frac{\alpha}{k} q_0 \int_{u=0}^{t_p} G^{\mathrm{S}}_{X21}(x,0,u) \int_{y'=0}^{L} G^{\mathrm{S}}_{Y11}(y,y',u)\,\mathrm{d}y' \\ & \times \int_{z'=0}^{L} G^{\mathrm{S}}_{Z11}(z,z',u)\,\mathrm{d}z'\,\mathrm{d}u + \frac{\alpha}{k} q_0 \\ & \times \int_{u=t_p}^{t} G^{\mathrm{L}}_{X21}(x,0,u) \int_{y'=0}^{L} G^{\mathrm{L}}_{Y11}(y,y',u)\,\mathrm{d}y' \\ & \times \int_{z'=0}^{L} G^{\mathrm{L}}_{Z11}(z,z',u)\,\mathrm{d}z'\,\mathrm{d}u \end{aligned} \tag{4}$$

The superscript S on the Green's function symbols denotes the "short" cotime and the L denotes the "long" cotime. The short cotime Green's functions are derived using the Laplace transform and the long cotime forms are found using the SOV method. The subscripts on the Green's function symbols in Eqs. (3) and (4) indicate the 1D planar geometry and boundary condition kinds; notice that the subscripts are contained in the case number $X21B10$ $Y11B00$ $Z11B00T0$ identified previously.

The task is now to find the six different Green's functions (GFs) cited in Eq. (4). In the time-partitioning method, the short dimensionless cotime GFs are usually accurate for [7]:

$$0 < \frac{\alpha t_p}{L^2} \leqslant 0.05 \tag{5}$$

In this example of a cube, each side is of length L. More generally, the characteristic dimension used in Eq. (5) is the smallest of the three sides in a parallelepiped. Expressions in the form of Eq. (5) involving the square of a length is related to Kelvin's rule of the squares [11]. For the cube, the partition time is $t_p \leqslant 0.05L^2/\alpha$. Intrinsic verification is usually obtained when using various values of cotime less than this value of t_p although, depending on the accuracy desired, even larger values can sometimes be used.

The short cotime Green's functions in Eq. (4) are approximately given by [5]:

$$G^{\mathrm{S}}_{X21}(x,0,u) \approx \frac{1}{\sqrt{\pi\alpha u}} \left[\mathrm{e}^{-\frac{x^2}{4\alpha u}} - \mathrm{e}^{-\frac{(2L-x)^2}{4\alpha u}} \right] \tag{6}$$

$$\int_{y'=0}^{L} G^{\mathrm{S}}_{Y11}(y,y',u)\,\mathrm{d}y' \approx 1 - \mathrm{erfc}\left(\frac{y}{\sqrt{4\alpha u}}\right) - \mathrm{erfc}\left(\frac{L-y}{\sqrt{4\alpha u}}\right) + \mathrm{erfc}\left(\frac{L+y}{\sqrt{4\alpha u}}\right) + \mathrm{erfc}\left(\frac{2L-y}{\sqrt{4\alpha u}}\right) \tag{7}$$

and an equation, similar to Eq. (7) is given for the z-direction. When smaller dimensionless cotimes than that given by Eq. (5) such as 0.01, only the first term in Eq. (6) and the first three terms in Eq. (7) are needed.

The long cotime equations are exactly given by [5]:

$$G^{\mathrm{L}}_{X21}(x,0,u) = \frac{2}{L} \sum_{m=1}^{\infty} \mathrm{e}^{-\beta_m^2 \frac{\alpha u}{L^2}} \cos\left(\beta_m \frac{x}{L}\right), \quad \beta_m = \frac{2m-1}{2}\pi \tag{8}$$

$$\int_{y'=0}^{L} G^{\mathrm{L}}_{Y11}(y,y',u)\,\mathrm{d}y' = 4 \sum_{n=1}^{\infty} \mathrm{e}^{-\gamma_n^2 \frac{\alpha u}{L^2}} \frac{\sin\left(\gamma_n \frac{y}{L}\right)}{\gamma_n}, \quad \gamma_n = (2n-1)\pi \tag{9a}$$

$$\int_{z'=0}^{L} G^{\mathrm{L}}_{Z11}(z,z',u)\,\mathrm{d}y' = 4 \sum_{p=1}^{\infty} \mathrm{e}^{-\eta_p^2 \frac{\alpha u}{L^2}} \frac{\sin\left(\eta_p \frac{z}{L}\right)}{\eta_p}, \quad \eta_p = (2p-1)\pi \tag{9b}$$

Obtaining a closed-form expression for the integration over u for the short cotime components in Eq. (4) can be difficult while the long cotime component integration is straightforward. The simplest way to perform the short cotime integration is numerically [7].

The solution given by Eq. (4) can be written as

$$\begin{aligned} T(x,y,z,t) &= T^{\mathrm{S}}(x,y,z,t_p) + T^{\mathrm{L}}_{\mathrm{c.t.}}(x,y,z,u)\Big|_{u=t_p}^{t} \\ &= T^{\mathrm{S}}(x,y,z,t_p) - T^{\mathrm{L}}_{\mathrm{c.t.}}(x,y,z,t_p) + T^{\mathrm{L}}_{\mathrm{c.t.}}(x,y,z,t) \end{aligned} \tag{10}$$

where the short cotime component is given by

$$T^{\mathrm{S}}(x,y,z,t_p) = \frac{\alpha}{k} q_0 \int_{u=0}^{t_p} G^{\mathrm{S}}_{X21}(x,0,u) \int_{y'=0}^{L} G^{\mathrm{S}}_{Y11}(y,y',u)\,\mathrm{d}y' \times \int_{z'=0}^{L} G^{\mathrm{S}}_{Z11}(z,z',u)\,\mathrm{d}z'\,\mathrm{d}u \tag{11}$$

and the long cotime solution is obtained by substituting Eqs. (8) and (9) into the second-half of Eq. (4) and integrating; the two long cotime components in the second line of Eq. (10) use

$$T^{\mathrm{L}}_{\mathrm{c.t.}}(x,y,z,u) = -32\frac{q_0 L}{k}\sum_{m=1}^{\infty}\sum_{n=1}^{\infty}\sum_{p=1}^{\infty} \mathrm{e}^{-\phi^2_{mnp}\frac{\alpha u}{L^2}} \times \frac{\cos\left(\beta_m \frac{x}{L}\right)\sin\left(\gamma_n \frac{y}{L}\right)\sin\left(\eta_p \frac{z}{L}\right)}{\gamma_n \eta_p \phi^2_{mnp}},$$

$$\phi^2_{mnp} = \beta^2_m + \gamma^2_n + \eta^2_p,$$

$$\beta_m = \frac{2m-1}{2}\pi,$$

$$\gamma_n = (2n-1)\pi, \quad \eta_p = (2p-1)\pi \tag{12}$$

evaluated at the respective cotimes of t_p and t. Eq. (11) is evaluated numerically, after substituting Eqs. (6) and (7), in program Conduction3D [12]. If Eq. (12) is evaluated as $u \to 0$, the series converges very slowly. As a consequence, we wish to make $u = t_p$ as large as possible while still obtaining the desired accuracy.

It is relevant to note that Eq. (12) is the same transient expression that is derived using the standard SOV solution for the steady state component; see Section 3.

As $t \to \infty$ in Eq. (10), the last term on the right disappears and the steady state solution is obtained:

$$T(x,y,z,\infty) = T(x,y,z) = T^{\mathrm{S}}(x,y,z,t_p) - T^{\mathrm{L}}_{\mathrm{c.t.}}(x,y,z,t_p) \tag{13}$$

This equation suggests an IVM since the left side is independent of time while the right side is a function of the partition cotime. It is important to note that the two right side components of Eq. (13) are independent since one comes from the Laplace transform method and the other from the SOV method. Moving the partition cotime over the acceptable range (see Eq. (5)) should give precisely the same value (for a given number of significant figures), thus exhibiting intrinsic verification which is demonstrated below. The steady state component is the most difficult part of the solution to evaluate numerically since it converges algebraically as discussed in Section 3; however, using Eq. (13) is very efficient.

An example is now given using the program Conduction3D [12] which is available upon request from the first author and implements the time-partitioning concepts discussed herein. (Most of the computations in this paper are done using Matlab with about 15-digit accuracy but Conduction3D is a Fortran program written with double precision which also gives about 15-digit accuracy.) The point $(0, L/4, L/2)$ is considered and the steady state temperature is calculated using a sufficiently large dimensionless time which is any value greater than about 1.0. (This time is found by making the exponent in Eq. (12) less than -23 for $m = n = p = 1$.) Dimensionless partition cotimes starting at 0.04 and ending at 0.5 are displayed in Table 1. Steady state temperature and heat flux components are shown. For dimensionless partition cotimes equal to or less than 0.05, 10-digit accuracy is obtained. The temperature for dimensionless times of 0.04 and 0.05 is 0.2474957959 and the same value is obtained if smaller partition cotimes are used. (Actually, this steady state number is given in Table 2, which uses a steady state solution obtained using Eq. (16), except the last digit is "8" instead of "9." However, an even more accurate calculation using Eq. (16) gives a "9" as the last digit.) This repetition of the same numerical value in Table 1 is a demonstration of the IVM. The heat flux in the x-direction is known to be q_0. The heat flux in the z-direction is zero because of symmetry but it is actually calculated to be less than 1.0E−16, which is zero to machine accuracy for double precision arithmetic. As the partition cotimes increase, the accuracy of the computed temperature decreases because the approximations for the short cotime components in Eqs. (6) and (7) become less accurate at these larger cotimes. The error of the heat flux in the y-direction changes sign; see the last column of Table 1.

Table 1
Time-partitioning solutions for the cube problem (denoted $X21B10$ $Y11B00$ $Z11B00T0$) at the point $(0, L/4, L/2)$ for the steady state values using Conduction3D [12] which incorporates the first intrinsic verification method

$\frac{\alpha t_p}{L^2}$	$\frac{T(0,\frac{L}{4},\frac{L}{2})}{q_0 L/k}$	$\frac{q_x}{q_0}$	$\frac{q_y(0,\frac{L}{4},\frac{L}{2})}{q_0}$	$\frac{q_z}{q_0}$	Percent error in T	Percent error in q_y
0.04	0.2474957959	1.0	−0.3824344581	0.0	<1E−8	<1E−8
0.05	0.2474957959	1.0	−0.3824344581	0.0	<1E−8	<1E−8
0.06	0.247495796**0**	1.0	−0.382434458**6**	0.0	4E−8	1.3E−7
0.07	0.247495797**7**	1.0	−0.382434463**7**	0.0	7.3E−7	1.5E−6
0.08	0.247495**8**072	1.0	−0.382434491**7**	0.0	4.6E−6	8.8E−6
0.10	0.247495**9**319	1.0	−0.382434**8**376	0.0	5.5E−5	9.9E−5
0.15	0.247499**0**175	1.0	−0.382441**2**568	0.0	0.0013	0.0018
0.20	0.247**5**097810	1.0	−0.382**5**30304	0.0	0.0057	0.0049
0.30	0.247**5**515697	1.0	−0.382**5**10893	0.0	0.0225	0.0043
0.35	0.247**5**776498	1.0	−0.382**4**10945	0.0	0.0331	0.0017
0.40	0.247**6**051522	1.0	−0.382**4**293229	0.0	0.0442	−0.0013
0.50	0.247**6**697664	1.0	−0.382**3**888309	0.0	0.0703	−0.0119

Underlined digits are inaccurate.

It is instructive to plot the absolute values of the errors in the calculated values versus the dimensionless partition cotimes; see Fig. 1. The absolute value is used for location $(0, L/4, L/2)$ because the errors in q_y/q_0 change sign for the extended range shown in Fig. 1. (Notice the link in Fig. 1 and the last column of Table 1.) The errors in the steady state results of Table 1 decrease rapidly as the dimensionless partition time decreases below about 0.1. Fig. 1 shows that these errors decrease by a factor of about three orders of magnitude between the partition cotimes of 0.1 and 0.05 for both the temperature and the heat flux component q_y. If less accuracy is desired, such as to about one part in 10^5, the partition cotime can be increased to 0.15, but as indicated below, the saving in computation is modest compared to using the partition cotime of 0.05. Using a dimensionless partition cotime of about 0.05 produces extremely accurate results (10 significant figures) with moderate computation, which is discussed next.

In using Eq. (10) for computation, the short cotime component is unaffected by the choice of the cotime but the number of terms in the triple sum has the potential

Table 2
Steady state temperatures calculated using Eqs. (15) and (16)

$\frac{x}{L}$	$\frac{y}{L}$	$\frac{z}{L}$	$\left.\frac{T(x,y,z)}{q_0L/k}\right\|_{\text{Eq. (15)}}$	# terms Eq. (15)	$\left.\frac{T(x,y,z)}{q_0L/k}\right\|_{\text{Eq. (16)}}$	# terms Eq. (16)
0	0.01	0.5	0.0302289007	810,000	0.0302309502	210,565
0.01	0.01	0.5	0.0230258420	105,245	0.0230258420	210,565
0.125	0.01	0.5	0.0079689860	671	0.0079689860	210,565
0.25	0.01	0.5	0.0040823037	170	0.0040823037	210,565
0.5	0.01	0.5	0.0012515931	41	0.0012515931	210,565
0.75	0.01	0.5	0.0003668360	19	0.0003668360	210,565
0	0.125	0.5	0.1774348124	810,000	0.1774347116	1431
0.01	0.125	0.5	0.1677045191	105,245	0.1677045191	1431
0.25	0.125	0.5	0.0484114960	170	0.0484114960	1430
0.5	0.125	0.5	0.0151614299	41	0.0151614299	1430
0.75	0.125	0.5	0.0044622686	19	0.0044622686	1430
0	0.25	0.5	0.2474956449	810,000	0.2474957958	420
0.01	0.25	0.5	0.2376531342	105,245	0.2376531342	420
0.25	0.25	0.5	0.0845353980	170	0.0845353980	420
0.5	0.25	0.5	0.0276376108	41	0.0276376108	420
0.75	0.25	0.5	0.0082141471	19	0.0082141471	420
0	0.5	0.5	0.2902454941	810,000	0.2902456191	170
0.01	0.5	0.5	0.2803677127	105,245	0.2803677127	170
0.25	0.5	0.5	0.1119676622	166	0.1119676622	168
0.5	0.5	0.5	0.0383737143	41	0.0383737143	168
0.75	0.5	0.5	0.0115552540	19	0.0115552540	168

These results are for the second kind of intrinsic verification.

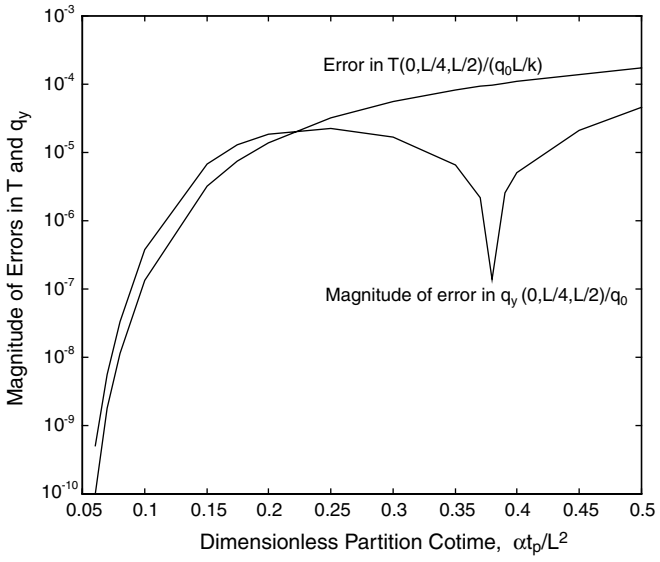

Fig. 1. Magnitude of errors as a function of the partition cotime in the steady state dimensionless temperature and heat flux in the y-direction at the point $(0, L/4, L/2)$. Results obtained using Conduction3D [12].

for much computation. A conservative way to determine maximum number of terms is to examine the exponential part of the complementary transient equation, Eq. (12). The condition of

$$\left[\left(\frac{2m-1}{2}\right)^2+(2n-1)^2+(2p-1)^2\right]\pi^2\frac{\alpha t}{L^2}\leqslant e_{\max} \qquad (14)$$

is used to determine the maximum number of terms in each of the summations. For $e_{\max}=23$ (since $\exp(-23)\approx 1.0\text{E}{-10}$) the maximum number of terms in the m-index is about 7 for $\alpha t/L^2=0.05$ and about 3 for both n and p, which are all relatively small, and thus efficient. (Actually the maximum numerical values are 7.18 for m and 3.80 for n and p; since only discrete values of m, n and p are used, values of 7 and 3 satisfy the accuracy requirement.) The upper limit of the number of terms in the triple product would then be 7 by 3 by $3=63$. The associated computational load in the triple summation is so small that it hardly needs reduction. Using a criterion of errors less than one part in 10^5 allows the $\alpha t/L^2=0.15$, from Fig. 1. This then allows replacing the value of $e_{\max}$ in Eq. (14) with 11.5. The result is a maximum value of m of 3 and the maximum for n and p of 1. Now the product of 3 by 1 by $1=3$ is certainly much less than 63 but the computer times for both 3 and 63 terms are negligible, particularly compared to some of the computations discussed below. This computation may even be insignificant compared to the computation for the numerical integration of the short cotime component in Eq. (10). A significant advantage of having a maximum of one term in two of the summations in Eq. (12) and only three terms in the other is that the triple summation reduces to a single summation containing only three terms.

When the time-partitioning method is used, two factors need to be considered. One is the value of the dimensionless partition cotime. If it is made too large, the approximations in the short cotime Green's functions given by Eqs. (6) and

(7) are not as accurate as needed. That is why the errors increase in Fig. 1 as the dimensionless partition cotime is made larger and is not monotonic above $\alpha t_p/L^2 \approx 0.2$. If the partition cotime satisfies Eq. (5), the errors are below about 1.0E−10, as shown in Fig. 1. The other factor is the number of terms required in the long cotime Green's functions; see Eq. (14).

3. The second IVM: steady state heat conduction solutions IVM

Without using the transient solution, several ways of verifying the steady state heat conduction solutions in parallelepipeds can be given. The method given here is to use different directions for the hyperbolic terms; the three directions of x, y and z are possible. The standard SOV solution has the hyperbolic terms in the non-homogeneous direction, which is the x-direction for the steady state version of the problem described by Eqs. (1) and (2). The notation for this problem is $X21B10$ $Y11B00$ $Z11B00$. The standard SOV solution is

$$T(x,y,z) = 16\frac{q_0 L}{k}\sum_{n=1}^{\infty}\sum_{p=1}^{\infty}\frac{\sinh\left(\phi_{np}\frac{L-x}{L}\right)}{\cosh(\phi_{np})}\frac{\sin\left(\gamma_n\frac{y}{L}\right)\sin\left(\eta_p\frac{z}{L}\right)}{\gamma_n\eta_p\phi_{np}} \tag{15a}$$

$$\gamma_n = (2n-1)\pi, \quad \eta_p = (2p-1)\pi, \quad \phi_{np} = \left[\gamma_n^2+\eta_p^2\right]^{1/2} \tag{15b}$$

Since the hyperbolic functions in Eq. (15a) tend to infinity (except at $x = L$) as n and p increase, it is good practice to compute the hyperbolic functions as exponentials, such as

$$T(x,y,z) = 16\frac{q_0 L}{k}\sum_{n=1}^{\infty}\sum_{p=1}^{\infty}\frac{e^{-\phi_{np}\frac{x}{L}}-e^{-\phi_{np}\left(2-\frac{x}{L}\right)}}{1+e^{-2\phi_{np}}} \times \frac{\sin(\gamma_n y/L)\sin(\eta_p z/L)}{\gamma_n\eta_p\phi_{np}} \tag{15c}$$

This form of the solution reveals that rapid, exponential convergence is possible for all values of x/L except at or near zero. At $x = 0$, one of the exponential terms becomes one and the Fourier series converges very slowly with terms $O(\gamma_n^{-3/2}\eta_p^{-3/2})$, making it unsuitable for computation. If the heat flux components are found from Eq. (15c) and evaluated at $x = 0$, the convergence is even slower than for the temperature.

Other forms of the solution can be found in various ways including steady state Green's functions and variation of parameters. The solution can also be found using separation of variables by finding the correction to a 1D steady state problem of $X21B10$ which has a simple solution of $T = q_0(L-x)/k$, $0 < x < L$. The resulting solution is

$$T(x,y,z) = \frac{q_0 L}{k}\frac{L-x}{L} - 4\frac{q_0 L}{k}\left\{\sum_{m=1}^{\infty}\sum_{p=1}^{\infty}\frac{\cos\left(\beta_m\frac{x}{L}\right)\cosh\left(\phi_{mp}\frac{L-2y}{L}\right)\sin\left(\eta_p\frac{2z}{L}\right)}{\cosh\left(\phi_{mp}\right)\beta_m^2\eta_p} + \sum_{m=1}^{\infty}\sum_{n=1}^{\infty}\frac{\cos\left(\beta_m\frac{x}{L}\right)\sin\left(\gamma_n\frac{2y}{L}\right)\cosh\left(\phi_{mn}\frac{L-2z}{L}\right)}{\cosh(\phi_{mn})\beta_m^2\gamma_n}\right\} \tag{16a}$$

$$\beta_m = (2m-1)\pi/2, \quad \gamma_n = (2n-1)\pi/2, \quad \eta_p = (2p-1)\pi/2$$
$$\phi_{mp} = \left[\beta_m^2/4+\eta_p^2\right]^{1/2}, \quad \phi_{mn} = \left[\beta_m^2/4+\gamma_n^2\right]^{1/2} \tag{16b}$$

For computational purposes the hyperbolic functions should be written in terms of exponentials. This equation has slow convergence at $y = 0$, L and $z = 0$, L but rapidly converges at $x = 0$ away from these y and z boundaries.

Table 2 displays temperature and heat flux results for the forms of the steady solution given by Eqs. (15) and (16). Values of x/L from 0 to 0.75 are given along with y/L values of 0.01–0.5. The z/L value is 0.5 so symmetry in y and z permits results for other (y,z) pairs. In addition to the locations of the points and numerical values for both equations, the total numbers of terms in the summations are given. For each location displayed except at $x/L = 0$, convergence is obtained and values accurate to 10 decimal places are given; the number of terms is found by requiring that the smaller magnitude exponent, as $\phi_{np}x/L$, in Eq. (15c), be less than 23. This criterion cannot be used for Eq. (15c) for $x = 0$; for that location an enormous number of terms may be needed. In Table 2 the number of terms for Eq. (15c) at $x = 0$ is limited to 900 in each summation, giving a total of 810,000 which is still not sufficient for 10-digit accuracy. The important point from the intrinsic verification perspective is that the use of two distinctly different expressions gives the same numerical values, at least to 10 decimal places, provided the computations are for points distant from critical locations, namely $x = 0$ for Eq. (15c) and $y = 0$, L and $z = 0$, L for Eq. (16). From a computational viewpoint, the two different solutions are complementary since between the two of them all points (except $x = y = 0$) can be accurately and efficiently treated. See also [13–15].

4. The third IVM: complementary transient solution IVM

The third type of intrinsic verification avoids the use of the short cotime component of the solution given by Eq. (13); hence, the numerical integration of the short cotime portion of the solution is not needed. At least two different variations of this third IVM are possible. The first variation uses locations removed from the heated surface where negligible temperature rise occurs for sufficiently small times. The second variation uses a one-dimensional semi-infinite solution in the time duration of its validity, which is larger than for the first variation. The second variation can be extended to 2D quarter-infinite solutions as well but that is left for future study.

4.1. IVM using zero temperature rise for $x > 0$ (first variation)

Consider now the first variation of the third type IVM. For interior locations not near the heated surface, only the large cotime component, $T^{L}_{c.t.}$, must be used. Introducing the steady state given by Eq. (13) into Eq. (10) gives the relation:

$$T(x,y,z,t) = T(x,y,z,\infty) + T^{L}_{c.t.}(x,y,z,t) = T(x,y,z) + T^{L}_{c.t.}(x,y,z,t) \quad (17)$$

For a sufficiently small dimensionless time and at an interior location, the temperature rise is negligible so that Eq. (17) gives

$$T(x,y,z,t) = 0 \approx T(x,y,z) + T^{L}_{c.t.}(x,y,z,t), \quad \alpha t/x^2 < C_0 \quad (18)$$

where the value of the dimensionless cutoff cotime, C_0, is to be determined. Replacing the inequality in Eq. (18) by an equality and solving for the steady state component gives

$$T(x,y,z) = -T^{L}_{c.t.}(x,y,z,t_0 = C_0 x^2/\alpha) \quad (19)$$

This equation suggests the third type (first variation) of the IVM. We have the steady state expression on the left which is a function of only position while on the right side is the negative of the complementary transient, a function of position and time. This expression can only be correct if the right side gives the same numerical value for all acceptable times. Hence we can verify the solution by examining numerical values with times less than indicated in Eq. (19).

Consider determination of the temperature in the cube with the same boundary conditions as considered above. Table 3 shows results for the complementary transient temperature equation, Eq. (12), evaluated at $y = z = L/2$ with $x = L/4$, $L/2$ and $3L/4$. The upper section of Table 3 is for $e_{max} = 23$ and the lower is for $e_{max} = 5$. The first column contains the dimensionless cotime and the third column contains the number of terms used in Eq. (12). Note that the same numerical values are repeated in Table 3 for sufficiently small cotimes; this is also illustrated by Fig. 2 which shows constant values for the smallest cotimes. For example, for $x = L/2$ and $e_{max} = 23$, the temperature value of -0.0383737143 is repeated five times in Table 3 for $0 < \alpha u/L^2 \leqslant 0.003$. See also Fig. 2 which shows a constant value of $T_{c.t.}$ for $\alpha u/L^2$ from 0 to about 0.02. (Times of 0.003 and 0.02 are quite different because the first is for changes of about 1.0E−10 and the other for changes of about 0.001.) For $x = 3L/4$, the number of repeated values in Table 3 is more and at $x = L/4$, it is less. The repeated values in each of these three cases demonstrate intrinsic verification. Note also that the $e_{max} = 23$ and small cotimes results of Table 3 are exactly the same values (except for the sign) as given in the last three rows of Table 2.

Several observations can be inferred from Table 3 and Fig. 2. One is that as the cotime goes to zero the negative of the complementary transient is equal to the steady state as given by Eq. (19). See Fig. 2 in which the lowest curve, $x/L = 1/4$, graphically shows the value going to the negative of its steady state value as the cotime goes to zero. However, the complementary transient need not be calculated at zero cotime. That is fortunate since the number of terms (column 3, Table 3) increases very rapidly as the cotime decreases below $\alpha u/L^2 = 0.003$, reaching 41,677 terms for $\alpha u/L^2 = 0.0005$ and $e_{max} = 23$. However, for the cases of $x/L = 1/4$, Table 3 indicates that no more than

Table 3
Steady state computation using the complementary transient solution, Eq. (12), at $y = z = L/2$

$\frac{\alpha u}{L^2}$	e_{max}	Number of terms	$x/L = 0.25$	$x/L = 0.5$	$x/L = 0.75$
0.0005	23	41,677	−0.1119676622	−0.0383737143	−0.0115552540
0.00075	23	22,693	−0.1119676622	−0.0383737143	−0.0115552540
0.001	23	14,732	−0.1119676621	−0.0383737143	−0.0115552540
0.002	23	5210	−0.1119665495	−0.0383737143	−0.0115552540
0.003	23	2837	−0.1119417544	−0.0383737143	−0.0115552540
0.005	23	1311	−0.1115668350	−0.0383737036	−0.0115552540
0.0075	23	722	−0.1101068425	−0.0383725039	−0.0115552540
0.01	23	458	−0.1075925258	−0.0383593742	−0.0115552512
0.02	23	165	−0.0920573779	−0.0375937451	−0.0115471326
0.05	23	42	−0.0476534588	−0.0267728927	−0.0102416604
0.1	23	15	−0.0150814189	−0.0103727386	−0.0049981466
0.25	23	3	−0.0005243432	−0.0003991574	−0.0002148549
0.0005	5	4235	−0.1119668019	−0.0383732736	−0.0115546610
0.00075	5	2296	−0.1119677350	−0.0383738032	−0.0115549641
0.001	5	1493	−0.1119635052	−0.0383737701	−0.0115563787
0.002	5	528	−0.1119616649	−0.0383717430	−0.0115532430
0.003	5	285	−0.1119450202	−0.0383793235	−0.0115552484
0.005	5	134	−0.1115793332	−0.0383842525	−0.0115551172
0.0075	5	73	−0.1100820514	−0.0383690887	−0.0115602187

This table illustrates the third kind (first variation) of intrinsic verification based on Eq. (19) which gives the steady state as the negative of these values as the dimensionless cotime is made smaller.

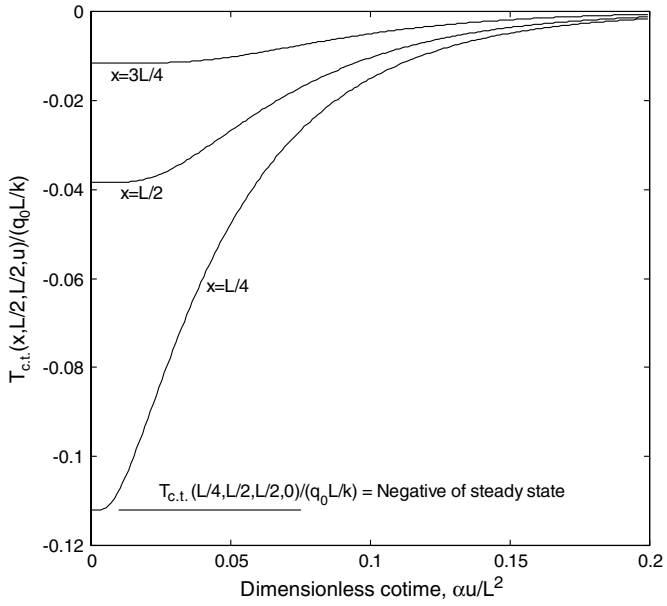

Fig. 2. Complementary transient temperatures for $x/L = 1/4$, 1/2 and 3/4 for $y = L/2$ and $z = L/2$ for the $X21B10\ Y11B00\ Z11B00T0$ problem. Notice the values at $u = 0$ give the negative of the steady state temperatures.

22,693 terms are needed. This number is still large but it can be reduced by a factor of about 10 using $e_{\max} = 5$ if four significant figure accuracy is satisfactory; see the lower section of Table 3.

The number of terms for complementary transient equation, Eq. (12), is shown in Fig. 3 for $e_{\max} = 5$, 11.5 and 23. As the dimensionless cotime ($\alpha u/L^2$) increases, the number of terms decreases rapidly. The decrease is shown to be a straight line in the log–log plot of Fig. 3. An approximate equation in the region $11.5 < e_{\max} < 23$ is

$$\log(N) = -\log(\alpha u/L^2) + 0.03922 e_{\max} - 1.234 \tag{20}$$

which is restricted to $\alpha u/L^2$ less than about 0.1. Fig. 3 is for any location in the cube but the dimensionless cotime for this first variation of the third IVM does depend on the location as indicated by Eq. (18). The errors in the computation of the complementary transient temperature also depend upon the location. See Fig. 4 which shows the errors for the location of ($L/4$, $L/2$, $L/2$). The maximum error in the $e_{\max} = 11.5$ solution is about 1.0E−7 and for $e_{\max} = 5$, it is about 1.0E−4. These errors are different by a factor of about 1000 but the difference in the number of terms is only about a factor of 3. Also these errors are much smaller than the $\exp(-e_{\max})$ values of 1.0E−5 and 0.0067 for $e_{\max} = 11.5$ and 5, respectively. The curves in Fig. 4 are somewhat "rough" because the sign changes a number of times which is not conveniently shown by the log–log plot. This "roughness" does not affect the monotonic behavior such as in Table 1 because the dominant error in Table 1 is caused by inaccuracy in the short cotime component, not the complementary transient components.

The cotime when the temperature no longer has negligible rise is approximately described by

$$\frac{\alpha t_0}{x^2} = C_0 = 0.013 \tag{21}$$

This is approximately the time when the temperature at x in a semi-infinite body with a constant heat flux at $x = 0$ just changes 10^{-10} compared to the temperature at $x = 0$. This problem is denoted $X20B1T0$ and has the solution

$$T_{X20B1T0}(x,t) = \frac{q_0}{k}(4\alpha t)^{1/2}\mathrm{ierfc}\left(\frac{1}{\sqrt{4\alpha t/x^2}}\right) \tag{22}$$

The temperatures at any time can be found using just the complementary transient values. For points away from the heated surface ($x = 0$ in this example), using Eqs. (17) and (19) gives the temperature as

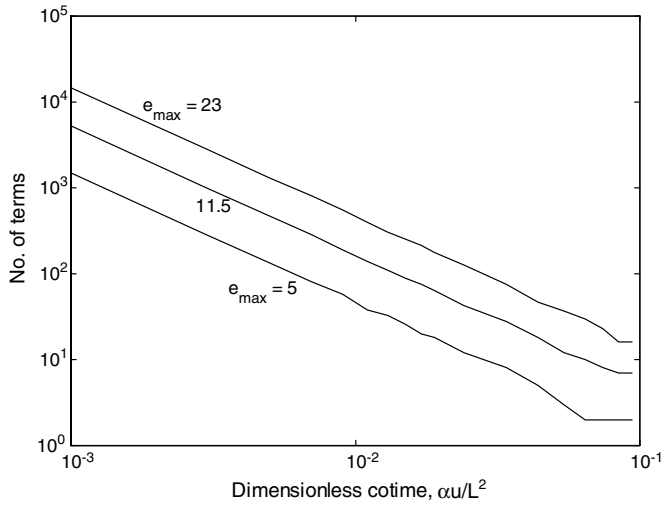

Fig. 3. Log–log plot of the number of terms for the complementary transient as a function of the dimensionless cotime, $\alpha u/L^2$, for Eq. (12) for $e_{\max} = 5$, 11.5 and 23.

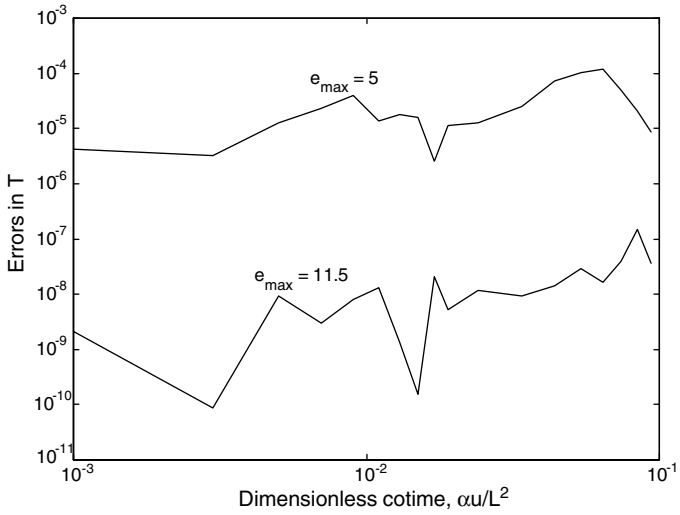

Fig. 4. Log–log plot errors in the computed complementary transient temperature at ($L/4, L/2, L/2$) as a function of the dimensionless cotime, $\alpha u/L^2$, for Eq. (12) for $e_{\max} = 5$ and 11.5.

$$T(x,y,z,t) = -T^{L}_{c.t.}(x,y,z,t = C_0 x^2/\alpha) + T^{L}_{c.t.}(x,y,z,t) \quad (23)$$

which gives the transient temperature as the difference of two complementary transient terms. A large number of terms may be needed for the first term on the right. See Fig. 5 for a plot of temperature using Eq. (23) for $x/L = 1/4$, 1/2 and 3/4 for $y/L = z/L = 1/2$. For plotting purposes, accuracy to 0.1% of the maximum temperature is quite satisfactory; in this case many fewer terms in the infinite series are needed than indicated in Table 3 and Figs. 3 and 4. If the $e_{max} = 23$ value in Eq. (14) is reduced to 5, the C_0 value in Eq. (23) can be increased from 0.013 to about 0.055 which also reduces the number of required terms in the summation. See the lower section of Table 3 which is for $e_{max} = 5$.

Intrinsic verification is possible regarding the eigenvalues and the number of terms in the summations. Consider first an error in the eigenvalues. Many types of errors are possible including inaccurate values, skipped values and values repeated erroneously. In research for 1D transient heat conduction problems with solid body flow [10], the IVM revealed that a solution was not correct; it was eventually learned that an eigenvalue was missing. In multi-layer multi-dimensional transient heat conduction problems, such as in [16], care must be exercised to avoid missing eigenvalues and calculating inaccurate values. Each error type will have the tendency to cause erratic or unexplained variations in the calculated temperatures as the dimensionless cotime is reduced.

Another possible error is using too few eigenvalues for the desired accuracy. Suppose that we replace the $e_{max} = 23$ in Eq. (14) with $e_{max} = 5$, but still expect about 10 digit accuracy. (Note that $\exp(-23) = 1.0\text{E}{-10}$ and $\exp(-5) = 0.0067$). The results are shown in the lower part of Table 3. Notice that the first few values for the $x/L = 1/2$ and 3/4 for $\alpha\, u/L^2 < 0.003$ keep changing at the sixth and seventh decimal places while we expect them to be invariant to 10 decimal places. (The errors do not vary monotonically because using the criterion given by Eq. (14) does not insure that.) The $e_{max} = 5$ and $\alpha u/L^2 < 0.003$ results in Table 3 are, however, invariant to five decimal places, which indicates the common values are accurate to that many decimal places. These are indications that the values are not accurate to 10 decimal places with $e_{max} = 5$ but are accurate to five decimal places.

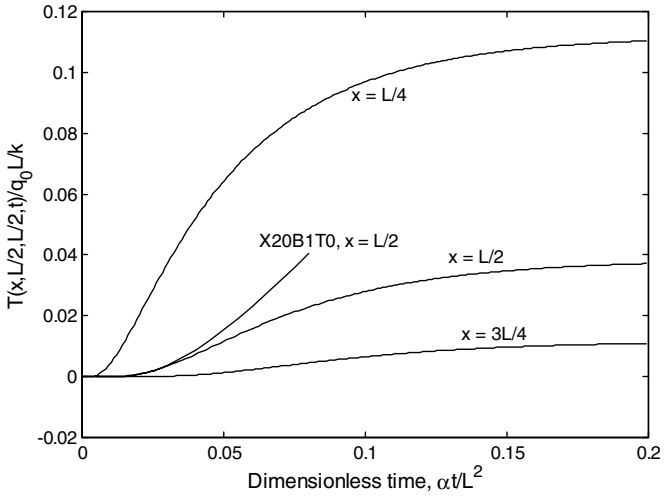

Fig. 5. Temperatures calculated using the complementary transient at locations $x/L = 1/4$, 1/2 and 3/4 and $y = z = L/2$. The semi-infinite solution at $x/L = 1/2$ is shown and denoted as $X20B1T0$.

4.2. Third IVM (second variation) using one-dimensional solution

Fig. 5 also shows the temperature at $x/L = 1/2$ using the 1D semi-infinite solution denoted $X20B1T0$ and given by Eq. (22); the close agreement between the 1D and 3D results suggests that the 1D curve can be applied for even larger cotimes than used just above, for plotting purposes up to about $\alpha t/L^2 = 0.03$ in Fig. 5 for $x/L = 1/2$. This observation leads to the second variation of this third IVM, as mentioned in the beginning of Section 4. Consider the case for $y \leqslant z \leqslant L/2$ and for 1D equivalent cutoff cotimes t_{1D} is such that

$$\frac{\alpha t_{1D}}{x^2 + y^2} < C_{1D} \quad (24)$$

where C_{1D} is a value identified later. Now x can be zero but both x and y cannot be simultaneously zero. Using the equality in Eq. (24) and use t_{1D} in Eq. (17) to get

$$T(x,y,z,t_{1D}) = T_{X20B1T0}(x,t_{1D}) = T(x,y,z) + T_{c.t.}(x,y,z,t_{1D}) \quad (25)$$

which gives the steady state result of

$$T(x,y,z) = T_{X20B1T0}(x,t_{1D}) - T_{c.t.}(x,y,z,t_{1D}) \quad (26)$$

This is another expression which demonstrates intrinsic verification, with no time dependence on the left side but time dependence on the right. Moving the parameter t_{1D} over the acceptable range should give the same numerical values. Eq. (26) has an advantage over Eq. (19), which comes from the first variation of this third IVM. Note that Eq. (26) has two independent parts on the right side, both depending on t_{1D}. This is unlike Eq. (19) which has only one part on the right side. As a consequence, verifying the multiplying factor of -32 in Eq. (12) cannot be accomplished using Eq. (19) but is possible using Eq. (26).

Table 4 displays numerical values to illustrate this second variation of the third IVM. The dimensionless times based on L for these cases are found from

$$\frac{\alpha t_{1D}}{L^2} = C_{1D}\left[\left(\frac{x}{L}\right)^2 + \left(\frac{y}{L}\right)^2\right] = C_{1D}\left[\left(\frac{x}{L}\right)^2 + \frac{1}{4}\right] \quad (27)$$

Using Eq. (27) for the dimensionless cotime ($\alpha t_p/L^2$) in Eq. (14) determines the number of terms required in Eq. (12). See the three columns in Table 4 which shows that the number of terms varies with C_{1D} and x/L. To get values for the steady state accurate to at least 10 decimal places, $e_{max} = 23$ is used. For the locations $x/L = 1/4$, 1/2 and

Table 4
Steady state computation using the complementary transient solution at $y = z = L/2$ for $x/L = 1/4$, 1/2 and 3/4

C_{1D}	e_{max}	$\frac{T(\frac{L}{4},\frac{L}{2},\frac{L}{2})}{q_0 L/k}$	Number of terms	$\frac{T(\frac{L}{2},\frac{L}{2},\frac{L}{2})}{q_0 L/k}$	Number of terms	$\frac{T(\frac{3L}{4},\frac{L}{2},\frac{L}{2})}{q_0 L/k}$	Number of terms
0.0128	23	0.1119676622	1846	0.038373714	908	0.0115552540	437
0.013	23	0.1119676622	1795	0.038373714	889	0.0115552540	433
0.0132	23	0.1119676623	1762	0.038373714	869	0.0115552540	418
0.0136	23	0.1119676623	1680	0.038373714	828	0.0115552540	399
0.014	23	0.1119676623	1614	0.038373714	799	0.0115552540	385
0.0142	23	0.1119676623	1574	0.038373714	778	0.0115552541	374
0.0144	23	0.1119676623	1534	0.038373714	765	0.0115552541	365
0.0148	23	0.1119676623	1485	0.038373714	735	0.0115552541	355
0.034	5	0.1120	42	0.0384	20	0.0116	11
0.036	5	0.1120	38	0.0385	18	0.0116	10
0.038	5	0.1120	37	0.0384	18	0.0116	10
0.04	5	0.1120	37	0.0384	16	0.0117	8
0.044	5	0.1120	30	0.0384	15	0.0117	7
0.048	5	0.1120	26	0.0384	12	0.0117	7
0.05	5	0.1121	26	0.0385	12	0.0118	7
0.052	5	0.1121	23	0.0385	11	0.0117	5

This table illustrates the third type (second variation) of the IVM based on Eq. (26).

3/4 in Table 4, the C_{1D} values vary from about 0.013 for $x/L = 1/4$–0.0144 for $x/L = 1/2$; this is not a large range. A conservative C_{1D} value for each of these x/L values is thus about $C_{1D} = 0.013$ for 10-digit accuracy. The number of terms required for the $x/L = 1/4$ location is about 1800 (fourth column of Table 4) which is a big improvement over the large value of 22,693 terms shown in Table 3 (first variation of the third IVM). This is a significant saving in computation. A more important point is that both methods give the same answer and both contain intrinsic verification, although the second variation is more powerful since the magnitude of the multiplying factor is verified.

If fewer significant figures are desired, such as the common engineering accuracy of three or four significant figures, the computation becomes more efficient but still intrinsic verification is possible. From Fig. 4 with $e_{max} = 5$, the errors are less than about 0.0001 which is consistent with the $e_{max} = 5$ results displayed in Table 4. In both the $x/L = 1/2$ and 3/4 cases, the digit in the fourth place fluctuates slightly. For example, for $x/L = 1/2$ and $C_{1D} = 0.034$, the dimensionless temperature is 0.0384 and the next C_{1D} value of 0.036 the value is 0.0385. After that the value reverts to 0.0384 until $C_{1D} = 0.05$. The correct values to four decimal places are given at $C_{1D} = 0.0384$ for the $e_{max} = 5$ values in Table 4, as can be verified by comparing the values to those for $e_{max} = 23$ in the same table. We conclude that this second variation of the third IVM can be used to verify solutions at a modest number of significant figures as well as with as many as 10 figures.

A further variation to use 2D solutions such as, $X20B1$ $Y10B0T0$ [9] is possible but is beyond the scope of this paper. Such solutions are efficient particularly near the $y = 0$ boundary at $x = 0$. However, the primary purpose of this paper is to demonstrate intrinsic verification, not to explore the computational advantages of each IVM. That is a topic for future exploration.

5. Conclusions

Intrinsic verification of heat conduction solutions in linear problems with simple geometries and boundary conditions is demonstrated. Intrinsic verification refers to the utilization of at least two independent exact solutions and obtaining numerical values to a specified number of significant figures compared to the heated surface. Although exact solutions can be symbolically checked by insuring that the describing partial differential equation, boundary conditions and initial condition are all satisfied, this does not guarantee that numerical values are accurate. Eigenvalues may be inaccurate or certain eigenvalues may be missing. Also an insufficient number of terms may be taken in the infinite series. Intrinsic verification can determine if such problems are present.

Three types of intrinsic verification are presented. The first is based on time partitioning for transient solutions. This method has a partition time (or cotime) which when varied over an acceptable range gives the same numerical value. This method has been successfully used to check thousands of cases when developing a transient heat conduction computer program [7]. The second method applies to steady state multi-dimensional problems; it uses independent solutions [13,14]. The third type of intrinsic verification avoids the numerical integration in the first IVM. This method can provide insight into the components of the solution. Each method has its unique advantages but the first and third types have the advantage of being useful in transient as well as steady state problems.

Extension of intrinsic verification to other geometries, such as cylindrical, in heat conduction is possible. Furthermore it may be possible in many other linear problems besides Fourier heat conduction, such as the telephone equation [17, p. 330], the hyperbolic heat conduction equation [5, p. xxvii] and others. It might even prove to be

possible to find intrinsic verification in solutions for certain nonlinear problems.

Acknowledgement

The authors appreciate the significant comments and insights of Dr. Arafa Osman.

References

[1] P.J. Roach, Verification and Validation in Computational Science and Engineering, Hermosa, Albuquerque, NM, 1998, Chapters 3–8.
[2] P. Knupp, K. Salari, Verification of Computer Codes in Computational Science and Engineering, Chapman & Hall/CRC, Washington, DC, 2003.
[3] R.L. McMasters, Z. Zhou, K.J. Dowding, C. Somerton, J.V. Beck, Exact solution for nonlinear thermal diffusion and its use for verification, AIAA J. Thermophys. Heat Transfer 16 (2002) 366–372.
[4] H.S. Carslaw, J.C. Jaeger, Conduction of Heat in Solids, second ed., Oxford Press, NY, 1959.
[5] J.V. Beck, K.D. Cole, A. Haji-Sheikh, B. Litkouhi, Heat Conduction Using Green's Functions, Hemisphere Publishing, Washington, DC, 1992.
[6] D.H.Y. Yen, J.V. Beck, R.L. McMasters, D.E. Amos, Solution of an initial-boundary value problem for heat conduction in a parallelepiped by time partitioning, Int. J. Heat Mass Transfer 45 (2002) 4267–4279.
[7] R.L. McMasters, K. Dowding, J.V. Beck, D.H.Y. Yen, Methodology to generate accurate solutions for verification in transient three-dimensional heat conduction, J. Numer. Heat Transfer (B) 41 (2002) 521–541.
[8] J.V. Beck, R.L. McMasters, Verification solutions for heat conduction with solid body motion and isothermal boundary conditions, Arab. J. Sci. Eng. 27 (2002) 49–65.
[9] J.V. Beck, A. Haji-Sheikh, D.E. Amos, D.H.Y. Yen, Verification solution for partial heating of rectangular solid, Int. J. Heat Mass Transfer 47 (2004) 4243–4255.
[10] J.V. Beck, R.L. McMasters, Solutions for multi-dimensional transient heat conduction with solid body motion, Int. J. Heat Mass Transfer 47 (2004) 3757–3768.
[11] C.R. MacCluer, Boundary Value Problems and Fourier Expansions, Revised ed., Dover Publications, Mineola, NY, 2004.
[12] J.V. Beck, Test cases for program V2000A and subroutine Conduction3D, Beck Engineering Consults Co. for Sandia National Labs., June 2002. Available from: <http://www.beckeng.com>.
[13] D.H.Y. Yen, J.V. Beck, Green's functions and three-dimensional steady state heat-conduction problems in a two-layered composite, J. Eng. Math. 49 (2004) 305–319.
[14] P.E. Crittenden, K.D. Cole, Fast-converging steady-state heat conduction in the rectangular parallelepiped, Int. J. Heat Mass Transfer 45 (2002) 3585–3596.
[15] K.D. Cole, Green's Function Library. Available from: <www.engr.unl.edu/~glibrary>.
[16] A. Haji-Sheikh, J.V. Beck, Temperature solution in multi-dimensional multi-layer bodies, Int. J. Heat Mass Transfer 45 (2002) 1865–1877.
[17] C.R. Wylie, Advanced Engineering Mathematics, fourth ed., McGraw-Hill Book Co., NY, 1975.